

# ACOUSTIC MODELING USING THE ULTRA WEAK VARIATIONAL FORMULATION

*Tomi Huttunen, Jari P. Kaipio*

University of Kuopio  
Department of Applied Physics  
P.O.Box 1627 FIN-70211 Kuopio, Finland  
tomi.huttunen@uku.fi  
jari.kaipio@uku.fi

*Peter Monk*

University of Delaware  
Department of Mathematical Sciences  
Newark, DE 19716  
USA  
monk@math.udel.edu

## ABSTRACT

Finite element methods (FEM) are widely used for the modeling of acoustic fields characterized by the Helmholtz equation. At high frequencies, however, the requirement of a sufficiently large number of elements per wavelength in standard FEM, may lead to an intolerable computational burden. Recently, a variety of new methods have been proposed that have the flexibility of FEM for general geometries while relax the need for dense meshes. One such method is the ultra weak variational formulation (UWVF). For the spatial discretization, the UWVF uses conventional finite element meshes but instead of polynomials used in FEM, the solution in each element is approximated using a system of plane waves. We show that a parallel UWVF method on a PC cluster can be used to simulate 3D acoustic fields that extend over tens of wavelengths.

## 1. INTRODUCTION

The Helmholtz equation is used to model a single frequency component of a steady-state acoustic pressure field. Standard tools for the full-wave modeling of the Helmholtz equation have been finite element methods (FEM) [11] and boundary element methods (BEM) [13]. In audio acoustics, applications of the Helmholtz equation range from the modeling interior acoustic fields [12] to the modeling of human auditory system [14]. Although FEM and BEM are well suited for low frequency problems, the requirement of a large number of elements per wavelength causes a rapid increase in the computational burden as the frequency increases. To extend the methods to higher frequencies, one is forced to use parallel computing techniques such as proposed in [3].

Recently, a variety of finite element type methods have been developed which try to relax the requirement for mesh density allowing the size of elements to be several wavelengths. In particular, methods that locally approximate the wave field using elementary solutions of the underlying Helmholtz problem (most commonly plane waves), have been a topic of intensive study. A review of this kind of improved methods can be found, for example, in [10]. An interesting example of these new methods is the ultra weak variational formulation (UWVF) proposed by Cessenat and Després [4, 5]. The method uses a new variational formulation over the element faces only (not over element volumes such as in FE methods). In addition, the discrete approximation of the UWVF is computed using plane wave basis functions in each element.

In this study, we show the feasibility of using the UWVF for audio acoustic simulations. In Section 2, we briefly outline the UWVF and its numerical approximation. The extension of the UWVF solution to the far-field is discussed in Section 3. In the numerical examples of Section 4, the UWVF method is applied for scattering of high frequency audio acoustic fields from a rigid obstacle. Finally, some conclusions are drawn in Section 5.

## 2. ULTRA WEAK VARIATIONAL FORMULATION

In this section we outline the coupled ultra weak variational formulation (UWVF) [5] and perfectly matched layer (PML) [2] method for the Helmholtz problem in an inhomogeneous medium. For a more detailed presentation of the method, we refer to [8, 10].

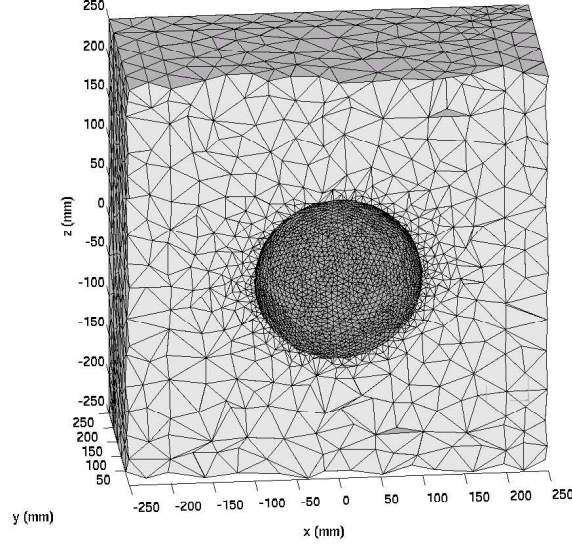


Figure 1: The partition of the computational domain using a tetrahedral finite element mesh. The mesh is used in the numerical simulations of Section 4.

We seek the solution of the time-harmonic pressure field  $P$  of the form

$$P(r, t) = p(r)e^{-i\omega t}, \quad (1)$$

where  $r = (x, y, z)$  is the spatial variable,  $t$  is time,  $p$  is the spatial dependent part of the field and  $\omega = 2\pi f$  is the angular frequency. We assume that the pressure  $p$  is the solution of the Helmholtz equation

$$\nabla \cdot \left( \frac{1}{\rho} \nabla p \right) + \frac{\kappa^2}{\rho} p = 0, \quad (2)$$

where  $\kappa = \omega/c + i\alpha$  is wave number and  $\rho$  is density. The complex valued wave number  $\kappa$  at frequency  $f$  is defined by the speed of sound  $c$  and absorption coefficient  $\alpha$ .

For the UWVF we partition the computational domain  $\Omega$  using a standard tetrahedral finite element mesh with elements  $K_k$ ,  $k = 1, \dots, N$ , see Fig.1. We denote the interface between two elements  $K_k$  and  $K_j$  by  $\Sigma_{k,j}$  and the face of element  $K_k$  on the exterior boundary of the mesh by  $\Gamma_k$ . The outward unit normal for the element  $K_k$  is  $n_k$ .

We assume that the mesh is chosen so that the parameters  $\rho$  and  $\kappa$  are constants in each element and we denote  $\rho_k \equiv \rho|_{K_k}$  and  $\kappa_k \equiv \kappa|_{K_k}$ . The Helmholtz problem for the acoustic pressure can be represented as a collection of

coupled problems so that for each element  $K_k$ ,  $k = 1, \dots, N$  we have

$$\nabla \cdot (A_k \nabla p_k) + \kappa_k^2 \eta_k^2 p_k = 0 \quad \text{in } K_k, \quad (3)$$

$$\frac{1}{\rho_k} n_k \cdot (A_k \nabla p_k) - i\varsigma p_k = -\frac{1}{\rho_j} n_j \cdot (A_j \nabla p_j) - i\varsigma p_j \quad \text{on } \Sigma_{k,j}, \quad (4)$$

$$\frac{1}{\rho_k} n_k \cdot (A_k \nabla p_k) + i\varsigma p_k = -\frac{1}{\rho_j} n_j \cdot (A_j \nabla p_j) + i\varsigma p_j \quad \text{on } \Sigma_{k,j}, \quad (5)$$

$$\left( \frac{1}{\rho_k} n_k \cdot (A_k \nabla p_k) - i\varsigma p_k \right) = Q \left( -\frac{1}{\rho_k} n_k \cdot (A_k \nabla p_k) - i\varsigma p_k \right) + g \quad \text{on } \Gamma_k, \quad (6)$$

where  $p_k = p|_{K_k}$ . The coupled transmission conditions (4) and (5) arise from the continuity of the acoustic pressure and normal particle velocity across element interfaces [1]. The coupling parameters  $\varsigma$  for (4) and (5) on the interface  $\Sigma_{k,j}$  and exterior boundary  $\Gamma_k$  are

$$\varsigma = \frac{1}{2} \left( \frac{\Re(\kappa_k)}{\rho_k} + \frac{\Re(\kappa_j)}{\rho_j} \right) \quad \text{and} \quad \varsigma = \frac{\Re(\kappa)}{\rho}, \quad (7)$$

respectively, where  $\Re(\kappa)$  is the real part of  $\kappa$ . On the exterior boundary the parameter  $Q \in \mathbb{C}$  with  $|Q| \leq 1$  is used for defining the boundary condition and  $g$  is the complex valued source function. Finally, the matrix  $A$  and the parameter  $\eta$  are either  $A = I$  and  $\eta = 1$  if the element is not in the PML or

$$A = \text{diag} \left( \frac{d_y d_z}{d_x}, \frac{d_x d_z}{d_y}, \frac{d_x d_y}{d_z} \right) \quad \text{and} \quad \eta^2 = d_x d_y d_z \quad (8)$$

if the element is in the PML. The parameters  $d_x$ ,  $d_y$  and  $d_z$  arise from the complex stretching of the spatial variables so that

$$\frac{\partial x'}{\partial x} = d_x \quad (9)$$

where

$$x' = \begin{cases} x + \frac{i}{\kappa} \int_{x_0}^x \sigma_0(|x| - x_0)^\nu dx, & |x| \geq x_0, \\ x, & |x| < x_0. \end{cases} \quad (10)$$

Similar expressions are used also for  $y$  and  $z$ . We also denote  $r' = (x', y', z')$ .

Instead of solving the pressure field  $p$  directly, a new function  $\chi_k$  is defined on element faces as follows

$$\chi_k = \left( \left( -\frac{1}{\rho_k} n_k \cdot (A_k \nabla) - i\varsigma \right) p_k \right) \Big|_{\partial K_k}, \quad 1 \leq k \leq N. \quad (11)$$

It is shown in [4, 5] that  $\chi_k$  satisfies the variational formulation

$$\begin{aligned} & \sum_{k=1}^N \int_{\partial K_k} \frac{1}{\varsigma} \overline{\chi_k \left( -\frac{1}{\rho_k} \frac{\partial}{\partial n_k} - i\varsigma \right) v_k} - \sum_{k=1}^N \sum_{j=1}^N \int_{\Sigma_{k,j}} \frac{1}{\varsigma} \overline{\chi_j \left( \frac{1}{\rho_k} \frac{\partial}{\partial n_k} - i\varsigma \right) v_k} \\ & - \sum_{k=1}^N \int_{\Gamma_k} \frac{Q}{\varsigma} \overline{\chi_k \left( \frac{1}{\rho_k} \frac{\partial}{\partial n_k} - i\varsigma \right) v_k} = \sum_{k=1}^N \int_{\Gamma_k} \frac{1}{\varsigma} \overline{g \left( \frac{1}{\rho_k} \frac{\partial}{\partial n_k} - i\varsigma \right) v_k}, \end{aligned} \quad (12)$$

for all piecewise smooth functions  $v_k$  satisfying the adjoint Helmholtz equation  $\nabla \cdot (A_k \nabla \bar{v}_k) + \kappa_k^2 \eta_k^2 \bar{v}_k = 0$  in  $K_k$ . Terms of the double summation in the second term on the left hand side are assumed to exist only if

two elements share a common face  $\Sigma_{k,j}$ . Equation (12) is called *the ultra weak variational formulation* of the Helmholtz problem.

The discrete UWVF is obtained by approximating the function  $\chi_k$  using complex conjugated plane wave basis functions

$$\chi_k^a = \sum_{\ell=1}^{N_k} \chi_{k,\ell} \left( -\frac{1}{\rho_k} n_k \cdot (A_k \nabla) - i\zeta \right) \varphi_{k,\ell}, \quad (13)$$

where

$$\varphi_{k,\ell} = \begin{cases} \exp(i\bar{\kappa}_k d_{k,\ell} \cdot r') & \text{in } K_k \\ 0 & \text{elsewhere,} \end{cases}$$

In addition, following the Galerkin method developed in [5], we choose  $v_k = \varphi_{k,\ell}$ . The angularly equidistributed directions  $d_{k,\ell}$  are obtained by minimizing the maximum distance between  $N_k$  points on the unit sphere [6]. In this study, the maximum allowed number of directions per element is limited to 130.

By substituting the plane wave approximation to the equation (12), the discrete UWVF problem can be written in the form of the matrix equation

$$(I - D^{-1}C)X = D^{-1}b. \quad (14)$$

The matrix  $D$  is a block diagonal matrix arising from the first term of (12). It consists of blocks  $D_k$ ,  $1 \leq k \leq N$  so that the block  $D_k$  corresponds to the element  $K_k$ . The sparse block matrix  $C$  couples the solution in a single element to adjacent elements or includes terms arising from the boundary conditions. The data vector  $b$  corresponds to the right hand side of (12) and the weights  $\chi_{k,\ell}$  form the vector  $X = (\chi_{1,1}, \chi_{1,2}, \dots, \chi_{N,N_k})$ . The parallelized method for choosing the number of basis functions  $N_k$  for each element and solving the matrix equation (14) is discussed in detail in [9, 10].

After the vector  $X$  is solved, the approximation of  $p_k$  in each element  $K_k$  can be computed as a direct summation

$$p_k = \sum_{\ell=1}^{N_k} \chi_{k,\ell} \varphi_{k,\ell}, \quad (15)$$

if  $\kappa_k \in \mathbb{R}$ . Otherwise, a simple post-processing step is required [8].

### 3. FAR-FIELD PATTERN

In many applications it is desirable to compute an approximation to the pressure  $p$  at a large distance from the sound source. To do this, we discuss briefly the computation of the far-field pattern from the UWVF approximation.

At a point  $r = (R, \theta, \phi)$  (given in spherical coordinates) at a large distance (i.e.  $R \gg 1$ ) from the scatterer, the field  $p$  can be decomposed into angular and radial parts so that

$$p(r) = \frac{e^{i\kappa R}}{R} p_\infty(\theta, \phi) + \mathcal{O}\left(\frac{1}{R^2}\right), \quad (16)$$

The angular part of the field is called *the far-field pattern* and it can be represented as [11]

$$p_\infty(\theta, \phi) = \frac{1}{4\pi} \int_S \left( p(r_S) \frac{\partial e^{-i\kappa r_0 \cdot r_S}}{\partial n} - \frac{\partial p(r_S)}{\partial n} e^{-i\kappa r_0 \cdot r_S} \right) dS, \quad (17)$$

where the surface  $S$  with outward normal  $n$  surrounds the scatterer,  $r_S$  is a point on  $S$  and  $r_0 = \frac{r}{|r|}$ .

The computation of the far-field pattern from the UWVF approximation relies on the following identity

$$\begin{aligned} & - \left( -\frac{1}{\rho} \frac{\partial p}{\partial n} - i\sigma p \right) \left( \frac{1}{\rho} \frac{\partial v}{\partial n} - i\sigma v \right) + \left( -\frac{1}{\rho} \frac{\partial v}{\partial n} - i\sigma v \right) \left( \frac{1}{\rho} \frac{\partial p}{\partial n} - i\sigma p \right) \\ & = 2i \frac{\sigma}{\rho} \left( p \frac{\partial v}{\partial n} - \frac{\partial p}{\partial n} v \right). \end{aligned} \quad (18)$$

Let us assume next that the surface  $S$  is constructed of the collection of the internal faces of the mesh, so that  $S = \cup_{n=1}^{N_S} \Sigma_{k,j}^n$ . Then, each face  $\Sigma_{k,j}^n$ ,  $1 \leq n \leq N_S$  is shared by two elements  $K_k$  and  $K_j$ . Let us also assume that element  $K_k$  has outward normal  $n_k = n$ . Consequently, for element  $K_j$  we get  $n_j = -n$ . By defining  $v = \exp(-i\kappa r_0 \cdot r_S)$ , using the definition (11) for  $\chi_k$  and  $\chi_j$ ; and with the help of the identity (18), the far-field pattern from the UWVF approximation can be computed via

$$p_\infty(\theta, \phi) = \frac{\rho}{8\pi i \sigma} \sum_{n=1}^{N_S} \int_{\Sigma_{k,j}^n} \left\{ \chi_j \left( -\frac{1}{\rho} \frac{\partial v}{\partial n_k} - i\sigma v \right) - \chi_k \left( \frac{1}{\rho} \frac{\partial v}{\partial n_k} - i\sigma v \right) \right\}, \quad (19)$$

where the integration is over all faces  $\Sigma_{k,j}^n$ ,  $1 \leq n \leq N_S$  that form the surface  $S$ . The discrete form of (19) is obtained by replacing  $\chi_k$  and  $\chi_j$  with their discrete approximations (13).

#### 4. ACOUSTIC SCATTERING PROBLEM

As a numerical example we investigate the scattering of an acoustic pressure field from a perfectly rigid sphere (radius  $a = 10$  cm) that is surrounded by an infinite, homogeneous medium. Rather than trying to imitate any particular application, this problem is chosen due to the existence of the analytical Fourier series solution [11] which allows us to evaluate the accuracy of the UWVF approximation. Similarly, it is also possible to derive an analytical solution for the far-field pattern. For this problem, the total field  $p$  can be divided into the sum of scattered  $p_s$  and incident fields  $p_i$  so that  $p = p_s + p_i$ . In this study, the incident field  $p_i(r) = A \exp(i\kappa d \cdot r)$  is a plane wave propagating in the direction of positive  $x$ -axis, i.e.  $d = (1, 0, 0)$ . The normal particle velocity is zero on the surface of the object  $\Gamma^{\text{obs}}$  which yields the boundary condition

$$\frac{\partial p_s}{\partial n} = -\frac{\partial p_i}{\partial n} \quad \text{on } \Gamma^{\text{obs}}. \quad (20)$$

Since we are seeking the UWVF approximation for the scattered field  $p_s$ , the exterior boundary condition (6) for the surface  $\Gamma^{\text{obs}}$  corresponds to (20) if we choose  $Q = 1$  and  $g = \frac{2}{\rho} \frac{\partial p_i}{\partial n}$ .

The sphere is embedded in air so we have  $\rho = 1.2$  kg/m<sup>3</sup> and  $c = 340$  m/s. Results are computed using the frequency  $f = 20$  000 Hz which corresponds to the wavelength  $\lambda = 1.7$  cm. Hence, we have  $\kappa a \approx 37.0$ . The computational domain in which the obstacles are enclosed is  $40 \times 40 \times 40$  cm cube surrounded by a 5 cm thick PML. The decay parameters in (10) are set to  $\sigma_0 = 30$  m<sup>-1</sup> and  $\nu = 0$ . On the exterior boundary of the PML we set  $Q = 0$  and  $g = 0$ .

The computer code used for the simulations is coded in Fortran90 and parallelized using MPI (Message Passing Interface). The computations are done with a Beowulf PC cluster consisting of 24 2.6 GHz Pentium 4 processors and having 48.0 GB total RAM. The processors are connected with a 1GB ethernet switch.

In Fig. 2 we show the UWVF approximations of scattered and total fields. A comparison with the Fourier series solution gives a relative error of 2.7% for the scattered field. The difference between the Fourier series solution and the UWVF approximation is shown in Fig. 3. The figure reveals that error is mainly originating from the surface of the scatterer. In fact, it is possible to improve the accuracy by refining the discretization near the sphere or using curved elements on the surface of scatterer. The latter approach has been used in 2D simulations in [7].

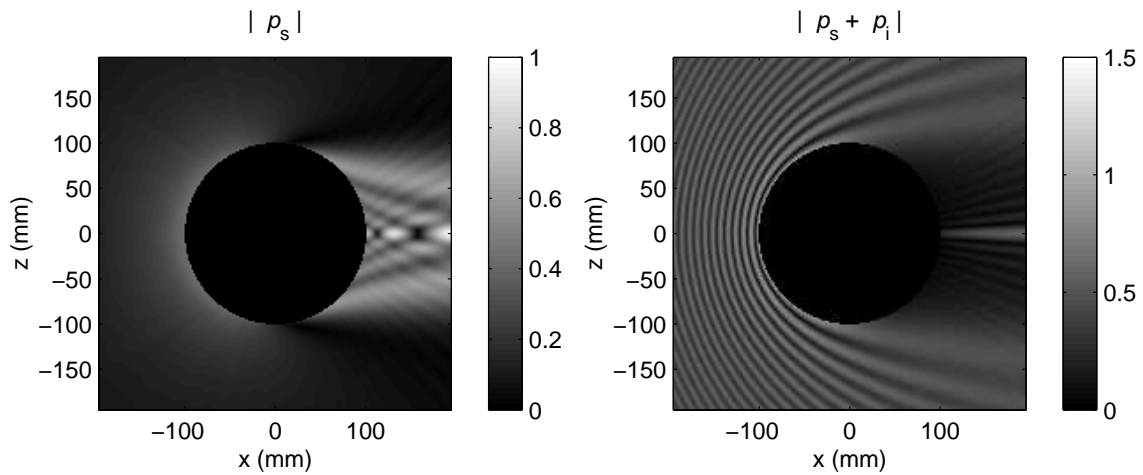


Figure 2: Scattered and total field for the scattering from the sphere problem. The error of the near field solution is 2.7 %

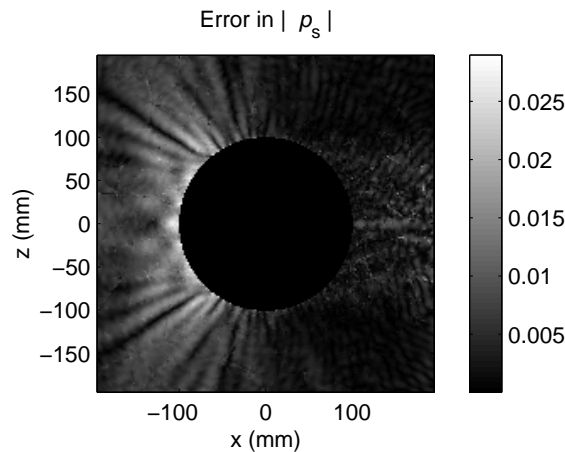


Figure 3: The difference field indicates that the major source of the error is the insufficiently large triangulation of the spherical surface.

The far-field pattern of the scattered field is shown in Fig. 4. Due to the relatively small error of the UWVF approximation, the lines for the exact solution and the UWVF approximation are hardly distinguishable from each other.

## 5. CONCLUSIONS

The aim of this study was to show that the parallel UWVF method can be used for simulating 3D audio acoustic Helmholtz problems in which the field extends over tens of wavelengths. Although the numerical example of this study is a field in a homogeneous medium, previous studies [7, 8, 10] show that the UWVF is also feasible for problems in inhomogeneous media. Therefore, the UWVF may offer potential advantages over boundary element methods whose complexity increases with the number of inhomogeneities within the computational domain. A benefit of the UWVF approach over standard finite element methods are much coarser meshes which reduce the computational burden.

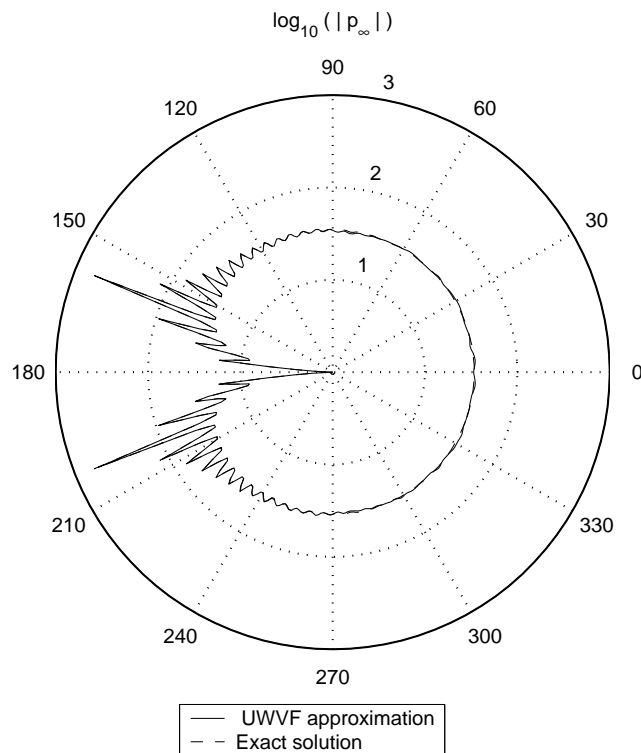


Figure 4: Polar plot of the far-field pattern for the scattered field from the sphere. The error of the UWVF approximation is 0.9 %, so the lines for exact and UWVF solutions can not be distinguished.

## 6. REFERENCES

- [1] J.D. Benamou and B. Després. A domain decomposition method for the Helmholtz equation and related optimal control problems. *Journal of Computational Physics*, 136:68–82, 1997.
- [2] J. Bérenger. A perfectly matched layer for the absorption of electromagnetic waves. *Journal of Computational Physics*, 114:185–200, 1994.
- [3] P. Geng, J.T. Oden and R.A. van der Geijn. Massively parallel computation for acoustical scattering problem using boundary element method. *Journal of Sound and Vibration*, 191(1):145–165, 1996.
- [4] O. Cessenat. *Application d'une nouvelle formulation variationnelle des equations d'ondes harmoniques, Problemes de Helmholtz 2D et de Maxwell 3D*. PhD thesis, Paris IX Dauphine, 1996.
- [5] O. Cessenat and B. Després. Application of an ultra weak variational formulation of elliptic PDEs to the two-dimensional Helmholtz problem. *SIAM Journal of Numerical Analysis*, 35(1):255–299, 1998.
- [6] R.H. Hardin, N.J.A. Sloane and W. D. Smith. Spherical coverings, May 1997. Available on: <http://www.research.att.com/~njas/coverings/index.html>.
- [7] T. Huttunen, P. Monk, and J.P. Kaipio. Computational aspects of the ultra-weak variational formulation. *Journal of Computational Physics*, 182:27–46, 2002.
- [8] T. Huttunen, J.P. Kaipio, and P. Monk. The perfectly matched layer for the ultra weak variational formulation of the 3D Helmholtz problem. *International Journal for Numerical Methods in Engineering*, 2004 Accepted.

- [9] T. Huttunen, P. Monk and J.P. Kaipio. Parallelized UWVF method for 3D Helmholtz problems *Proceeding of ECCOMAS*, July 24-28. 2004 Jyväskylä, Finland, Submitted.
- [10] T. Huttunen. *The ultra weak variational formulation for ultrasound transmission problems*. PhD thesis, University of Kuopio, 2004. Available on: <http://physics.uku.fi/~huttunen>
- [11] F. Ihlenburg. *Finite Element Analysis of Acoustic Scattering*. Springer, 1998.
- [12] S. Kopuz and N. Lalor. Analysis of interior acoustic fields using the finite element method and the boundary element method. *Applied Acoustics*, 45: 193-210, 1995
- [13] P.K. Kythe. *An Introduction to Boundary Element Methods*. CRC Press, 1995.
- [14] T. Walsh, L. Demkowicz and R. Charles. Boundary element modeling of the external human auditory system. *The Journal of the Acoustical Society of America*, 115(3):1033-1043, 2004